Field Emission of Carbon Nanotubes

Jisoon Ihm and Seungwu Han
Department of Physics and Center for Theoretical Physics
Seoul National University
Seoul 151-742, Korea

We have performed *ab initio* pseudopotential electronic structure calculations for various edge geometries of the (n,n) singlewall nanotube with or without applied fields. Among the systems studied, the one with the zigzag edge exposed by a slant cut is found to be the most favorable for the emission due to the existence of unpaired dangling bond states around the Fermi level. The next favorable geometry is the capped nanotube where π-bonding states localized at the cap and pointing to the tube axis direction occur at the Fermi level. A scaling rule of the induced field linear in the aspect ratio of the tube is also obtained.

I. INTRODUCTION

From the beginning of its discovery, the carbon nanotube (CNT) has been regarded as an ideal material to make field emitters because of its unusually high aspect ratio as well as mechanical and chemical stability. Many experiments with singlewall [1,2] and multiwall [3–7] carbon nanotubes have demonstrated a relatively low threshold voltage of the electron emission with little sample degradation. Recently, flat panel displays fabricated with the CNT's as emitters are demonstrated [8]. Furthermore, the advancements in fabrication technology make it possible to generate a self-aligned or a patterned CNT on a glass [9] or a silicon substrate [10], implying that a commercial production of the CNT-based field emission display (FED) may be possible in near future.

In spite of the accumulating experimental data, realistic quantum mechanical calculations on the field emission of the CNT are still scarce. The simplistic view of the CNT as a jellium metallic emitter based on the conventional Fowler-Nordheim theory could not explain the entire range of the I-V data [1,7] and a critical analysis of the electronic structure on a more fundamental level is required. In this study, we perform *ab initio* pseudopotential electronic structure calculations [11,12] with or without applied fields. We focus on the end geometries of the CNT where the electron emission actually occurs and try to find the optimized tip structure for field emission. Some of the results presented here have been submitted for publication elsewhere [13].

II. MODEL SYSTEM AND COMPUTATIONAL METHOD

We consider various end geometries of the CNT. The side views of the upper part of the (5,5) CNT's are shown in Fig. 1. The bottom (not shown) of the tube body is terminated with hydrogen atoms for computational convenience. We call (a)-(d) as H(hydrogen-attached)-, FC(flat-cut)-, CAP(capped)-, and SC(slant-cut)-CNT, respectively. The H-CNT represents a situation where the dangling bonds are chemically stabilized by ambient hydrogen. In the CAP-CNT model, the tube end is capped with a patch (hemisphere) of C_{60} having six pentagons. In the FC-CNT and SC-CNT, on the other hand, dangling bonds remain unsaturated. The model systems are periodically repeated in a tetragonal supercell with the tube axis lying in the z-direction. In order to make the simulation as realistic as possible, various computational schemes are adopted in this study.

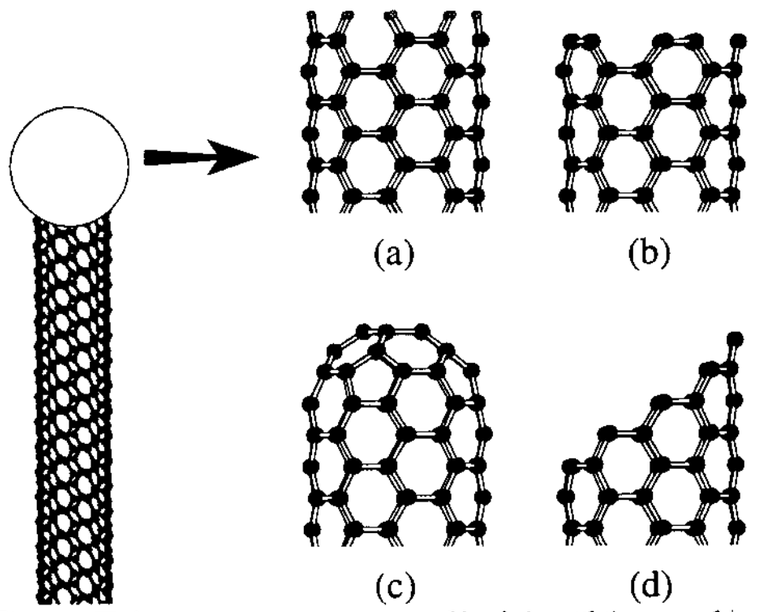

FIG. 1. Edge structures studied in this work. (a) H-CNT, (b) FC-CNT, (c) CAP-CNT, and (d) SC-CNT (see text for abbreviations).

The plane-wave based calculations have been done mostly for a $\sim 20\AA \times 20\AA \times 30\AA$ unit supercell. To check the convergence of our results for larger systems, we have also used localized basis functions [14] in the *ab initio* pseudopotential calculations and have been able to enlarge the tube size up to four times. The base grid of 60 Ry. is used for the projection of the orbital and wave function. Relaxed geometries are obtained from computationally less demanding tight-binding calculations [15].

III. ELECTRONIC STRUCTURE OF MODEL SYSTEMS

In Fig. 2, the total density of states (TDOS) around the Fermi level is plotted in solid lines. All sys-

tems except the H-CNT have localized states near the nanotube edge. To investigate these localized states more closely, the local density of states (LDOS) around the end region is calculated and shown in dashed lines in Fig. 2(b) and (c). Energy levels of the localized states induced by the topological defects (pentagons) in the CAP-CNT are known to depend on the relative positions between the defects [16–18] and the pentagons are assumed to be separated from each other here as found in Ref. 17. In Fig. 2(d), the LDOS of the SC-CNT at the two topmost atoms (the sharp edge) and that at the eight side atoms on the slant-cut cross section are shown in dotted and dashed lines, respectively. Descriptions about different characters of these two will be given in the following section. In the SC-CNT, localized π states predicted for the graphite ribbons [19] are also found, but they are less prominent than the σ-bond-derived states and unimportant to field emission.

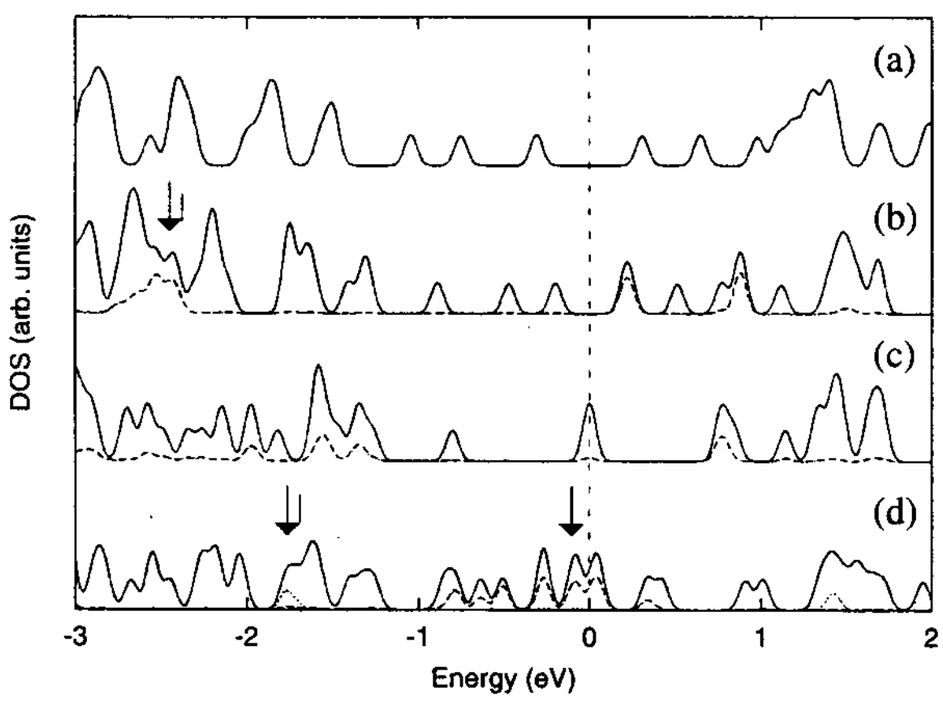

FIG. 2. TDOS (solid line) and LDOS (dashed or dotted lines) corresponding to each structure [(a)-(d)] in Fig. 1. The Fermi level is set to zero. The LDOS represents the states localized at the top of the nanotubes in Fig. 1. In (d), the dashed and dotted lines are differentiated as explained in the text.

In Fig. 3(a), we show one of the localized states in the FC-CNT whose energy level is indicated by an arrow in Fig. 2(b). Interestingly, two adjacent dangling bonds join at the backbond position of the original sp^2 configuration. The character of the s-orbital is slightly lost in the sp^2 hybridization. Because of these additional bonds, the C-C bond length in the top layer is 1.27$\AA$ compared with the ideal C-C distance in a perfect nanotube (1.41$\AA$), corresponding to a strong double bond. Two types of localized states are identified in the SC-CNT model. In Fig. 3(b), the topmost atoms on the armchair-like edge (states at -1.8 eV indicated by an arrow in Fig. 2(d)) show a similar backbonding as in the FC-CNT, while the individual dangling bonds on the side edge (indicated by an arrow at -0.1 eV in Fig. 2(d)) re-

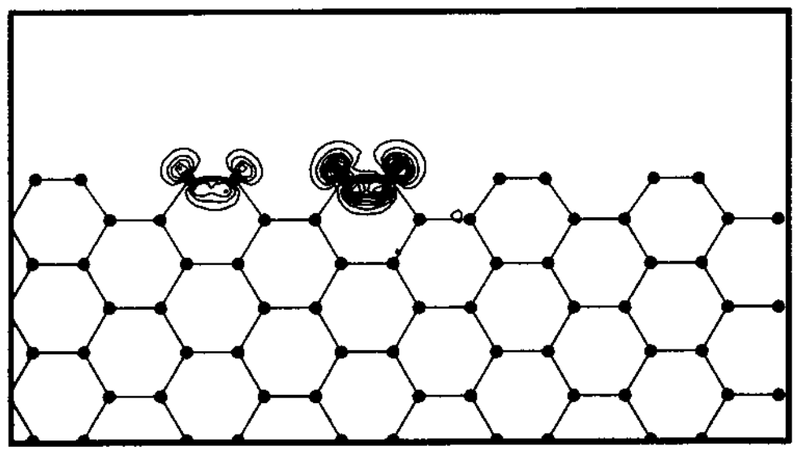

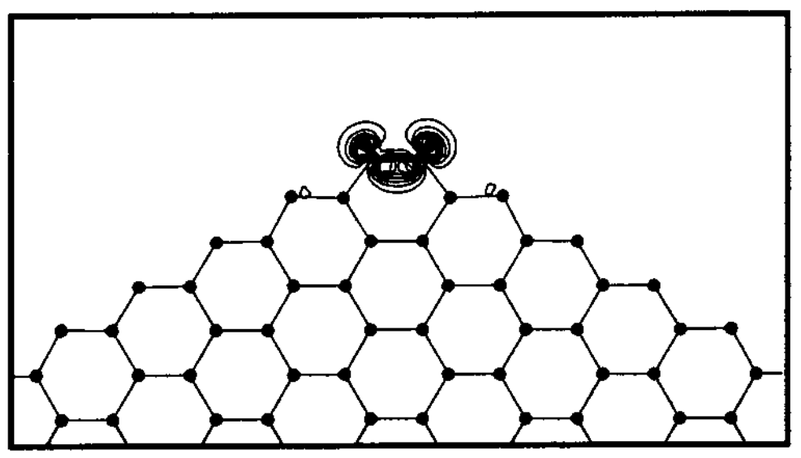

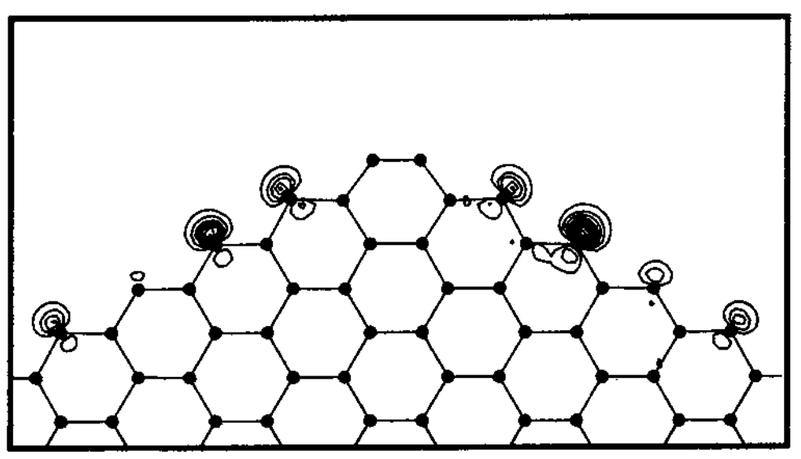

FIG. 3. Electron density of the localized states whose energy levels are indicated by arrows in Fig. 2(b) and (d). (a) is the localized state of the FC-CNT at -2.6 eV and (b) and (c) are the localized states of the SC-CNT at -1.8 eV and -0.1 eV, respectively. The electron density is evaluated on the nanotube surfaces and the contour interval is 0.08 $e/\AA^3$.

On the other hand, the energy splitting between the bonding and antibonding states is rather significant ($\sim$3 eV) for the states localized at the armchair edge as shown in two separate dotted curves.

IV. EFFECT OF EXTERNAL FIELDS

Now we examine the change in the electronic structure by the field in detail. In Fig. 4(a) shown above, the DOS for the SC-CNT under the applied field ($\sim$ 0.4 V/$\AA$) is plotted. Comparing it with Fig. 4(b) (the same as Fig. 2(d)) for the zero field case, we notice that the localized levels at the armchair edge (dotted

curves) undergo a downward shift. The states localized on the zigzag chain sides of the edge are partially occupied for the zero field in Fig. 4(b) (dashed curves) and their occupation increases as the field is turned on. Such a situation is commonly observed in the field emission of metallic tips with atomic adsorbates [20]. Since these states are located at the Fermi level under the applied field, they are the first to be emitted across the barrier to the anode. The increase in the occupation of the dangling bond states is approximately 0.1e per edge atom. The downward shift of the localized states by the field occurs in the FC-CNT and CAP-CNT as well. Shifts of the localized states are pinned as they begin to be occupied, hence these localized states stay at the Fermi level for a wide range of the field strength. The occupation of the localized states has an effect of repulsing the π-electrons and suppresses the increase in the amplitude of the π states at the edge. Actually, the sum of the accumulated charge does not vary too much from structure to structure.

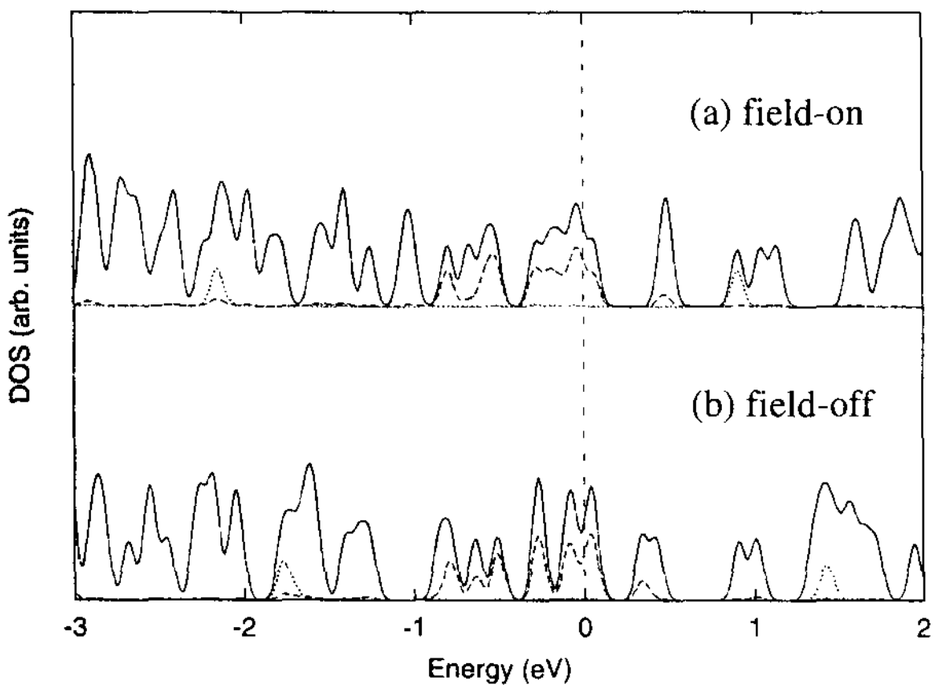

FIG. 4. Change in the DOS of the SC-CNT under the applied field $\sim$0.4 V/$\AA$. Solid lines are the total DOS. Dashed and dotted lines are the local DOS and they are differentiated as in Fig. 2(d).

V. FIELD EMITTER ARRAY

Another interesting issue we pursue here is the dependence of the field enhancement factor on the separation and packing of the nanotubes. We have already presented the results for an isolated nanotube and now show other cases. We have performed the same electronic structure calculations with the rope (infinite hexagonal array of nanotubes in the xy plane separated by 3.4 $\AA$ from each other with a finite length in z direction). The self-consistent electronic structures with and without the applied electric field are calculated and the induced charge is obtained. Then we calculate the field at the tube edge produced by an isolated tube with this induced charge, that produced by a (3×3) array of tubes (at the edge of the central tube), that by a (5×5) array of tubes, etc. Figure 5 shows the field obtained in this way and this plot implies two crucial effects. First, as the number of close-packed nanotubes increases, the field decreases. This is expected because the larger the packed area is, the more similar to the planar geometry (which does not enhance the field) is the configuration. The effective curvature of the tube at the edge is substantially reduced when the tubes form a rope. The converged value of E_{ind} in the large n limit here is only about a quarter of the field produced by a tube in the isolated configuration studied above. Secondly, the induced charge per tube in the rope configuration is also significantly diminished compared with that in the isolated case. The field for $n = 1$ in Fig. 5 is only about half of the corresponding field produced by the isolated tube under the some applied field. Therefore it is desirable to deposit (or grow) nanotubes far apart from each other for efficient field emission. The enhancement is effective if the separation between tubes is beyond a few nanometers. Another desirable, yet difficult thing to achieve is to have singlewall nanotubes rather than multiwall tubes. It is also found that the ratio of E_{ind} between CAP-CNT and H-CNT is significantly enlarged from that in the isolated situation, which implies that the effects of localized states and the shape of the end structure become more important in the close-packed configuration.

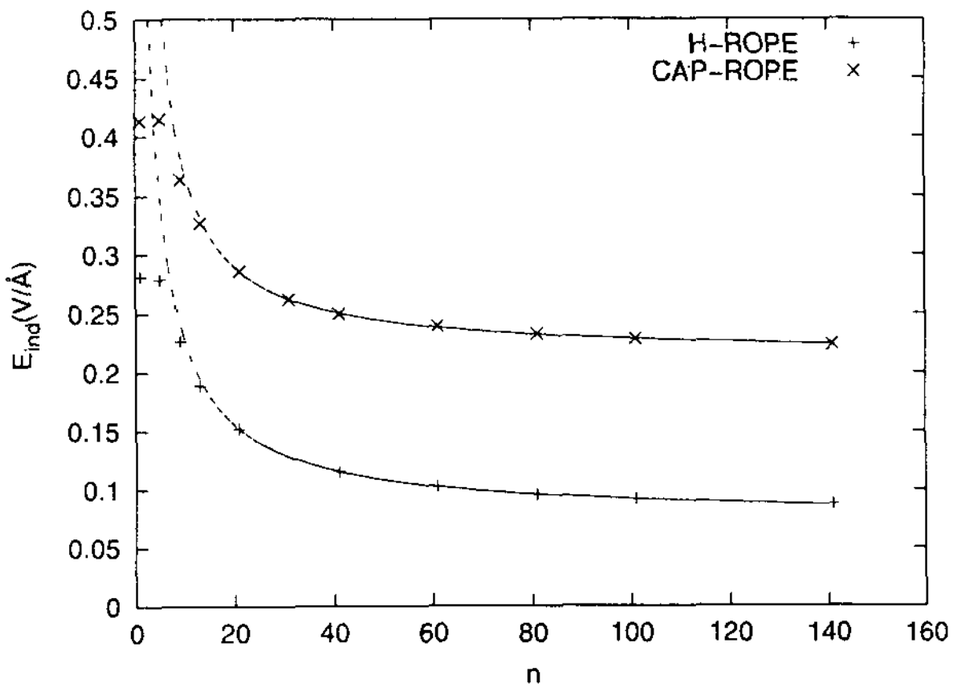

FIG. 5. The induced field by the $E_{appl} \approx 0.3$ V/$\AA$ at the edge of the central tube (40 $\AA$) in a rope. The abscissa is the number of close-packed tubes along a side of square that contribute to the field of the central tube. The asymptotic behavior is nicely fitted with the curve $a/(n-b)+a$.

VI. DISCUSSION

In summary, we have studied the electronic structure of various edge shapes of a singlewall nanotube

with or without external fields. A linear scaling behavior of the field enhancement factor as a function of the tube length has been obtained. Open tubes with dangling bonds at the zigzag-type edge are predicted to be the most favorable for the field emission among the structures considered here. The capped nanotubes with π-bonding states localized at the cap region are the next favorable structure. In a real situation, it is likely that hydrogen atoms or other ambient atoms and molecules cap the reactive dangling bonds of the open nanotubes. However, the attached atoms or molecules may be desorbed by an initial clean-up procedure before emission or by a strong local field during the emission process. Fortunately, the strong sp^2 bond of the tube body is not dissociated at all under the typical field ($\lesssim$ 1 V/Å) in experiment. For multiwall CNT cases, the saturated (3-fold) coordination of all edge atoms by bridging carbon atoms cannot occur in general because of the the incommensurability between neighboring coaxial tubes, and there should remain some unsaturated dangling bonds contributing actively to the field emission [21]. Existing experimental data do not yet give information on the dependence of the emission efficiency on the tip structure. Our study proposes a high-efficiency edge structure which can significantly improve the field emission performance. We also note that, for the practical display application, it is enough for only a small fraction of nanotubes to actually emit electrons because of huge redundancy in the total number of nanotube emitters.

Acknowledgment. - The study on the carbon nanotube field emitter array was supported by the Samsung Electronics.

REFERENCES

[1] Y. Saito, K. Hamaguchi, T. Nishino, K. Hata, K. Tohji, A. Kasuya, and Y. Nishina, Jpn. J. Appl. Phys. **36**, L1340 (1997).

[2] J.-M. Bonard, J.-P. Salvetat, T. Stockli, W. A. de Heer, Appl. Phys. Lett. **73**, 918 (1998).

[3] A. G. Rinzler, J. H. Hafner, P. Nikolaev, L. Lou, S. G. Kim, D. Tomanek, P. Nordlander, D. T. Colbert, and R. E. Smalley, Science **269**, 1550 (1995)

[4] W. A. de Heer, A. Chatelain, and D. Ugarte, Science **270**, 1179 (1995).

[5] Y. Saito, K. Hamaguchi, S. Uemura, K. Uchida, Y. Tasaka, F. Ikazaki, M. Yumura, A. Kasuya, and Y. Nishina, Appl. Phys. A **67**, 95 (1998).

[6] Q. H. Wang, T. D. Corrigan, J. Y. Dai, and R. P. H. Chang, Appl. Phys. Lett. **70** 3308 (1997).

[7] P. G. Collins and A. Zettl, Appl. Phys. Lett. **69**, 1969 (1996); P. G. Collins and A. Zettl, Phys. Rev. B **55**, 9391 (1997).

[8] Q. H. Wang, A. A. Setlur, J. M. Lauerhaas, J. Y. Dai, E. W. Seelig, and R. P. H. Chang, Appl. Phys. Lett. **72**, 2912 (1998); Y. Saito, S. Uemura, and K. Hamaguchi, Jpn. J. Appl. Phys. **37**, L346 (1998); W. B. Choi, D. S. Chung, S. H. Park, and J. M. Kim, in Proceedings of the MRS Spring Meeting, San Francisco (1999) and Appl. Phys. Lett. **75**, 3129 (1999).

[9] Z. F. Ren, Z. P. Huang, J. W. Xu, J. H. Wang, P. Bush, M. P. Siegal, and P. N. Provencio, Science **282**, 1105 (1998); S. Fan, M. G. Chapline, N. R. Franklin, T. W. Tombler, A. M. Cassell, and H. Dai, *ibid.* **283**, 512 (1999).

[10] S. Fan, M. G. Chapline, N. R. Franklin, T. W. Tombler, A. M. Cassell, and H. Dai, Science **283**, 512 (1999).

[11] J. Ihm, A. Zunger and M. L. Cohen, J. Phys. C:Solid State Phys., **12**, 4409 (1979).

[12] N. Troullier and J. L. Martins, Phys. Rev. B **43**, 1993 (1991).

[13] Seungwu Han and Jisoon Ihm (to be published).

[14] O. F. Sankey and D. J. Niklewski, Phys. Rev. B **40**, 3979 (1989); The r_C is set to 4.0 for C and H atoms.

[15] C. H. Xu, C. Z. Wang, C. T. Chan, and K. M. Ho, J. Phys.: Condens. Matter 4, 6047 (1992).

[16] D. L. Carroll, P. Redlich, P. M. Ajayan, J. C. Charlier, X. Blase, A. De Vita, and R. Car, Phys. Rev. Lett. **78**, 2811 (1997).

[17] P. Kim, T. W. Odom, J.-L. Huang, and C. M. Lieber, Phys. Rev. Lett. **82**, 1225 (1999); R. Tamura and M. Tsukada, Phys. Rev. B **52**, 6015 (1995).

[18] A. De Vita, J. -Ch. Charlier, X. Blase, and R. Car, Appl. Phys. A **68**, 283 (1999).

[19] M. Fujita, K. Wakabayashi, K. Nakada, and K. Kusakabe, J. Phys. Soc. Japan. **65**, 1920 (1996).

[20] V. T. Binh, S. T. Purcell, N. Garcia, and J. Doglioni, Phys. Rev. Lett. **69**, 2527 (1992); M. L. Yu, N. D. Lang, B. W. Hussey, T. H. P. Chang, and W. A. Mackie, Phys. Rev. Lett. **77**, 1636 (1996).

[21] J. Charlier, A. De Vita, X. Blase and R. Car, Science **275**, 646 (1997).